Higgs Radiation Off Top Quarks at the Tevatron and the LHC

W. Beenakker,[1] S. Dittmaier,[2] M. Krämer,[3] B. Plümper,[2] M. Spira,[4] and P. M. Zerwas[2]

[1]*Theoretical Physics, University of Nijmegan, NL-6500 Nijmegan, The Netherlands*
[2]*Deutsches Elektronen-Synchrotron DESY, D-22603 Hamburg, Germany*
[3]*Department of Physics and Astronomy, University of Edinburgh, Edinburgh EH9 3JZ, Scotland*
[4]*Paul Scherrer Institut PSI, CH-5232 Villigen PSI, Switzerland*

(Received 10 July 2001; published 29 October 2001)

Higgs bosons can be searched for in the channels $p\bar{p}/pp \to t\bar{t}H + X$ at the Fermilab Tevatron and the Cern Large Hadron Collider (LHC). We have calculated the QCD corrections to these processes in the standard model at next-to-leading order. The higher-order corrections reduce the renormalization and factorization scale dependence considerably and stabilize the theoretical predictions for the cross sections. At the central scale $\mu = (2m_t + M_H)/2$ the properly defined K factors are slightly below unity for the Tevatron ($K \sim 0.8$) and slightly above unity for the LHC ($K \sim 1.2$).

DOI: 10.1103/PhysRevLett.87.201805 PACS numbers: 14.80.Bn, 12.15.–y, 12.38.Bx, 13.85.–t

The search for Higgs bosons [1] is one of the most important experimental programs in high-energy physics. If successful, a crucial step in revealing the mechanism for electroweak symmetry breaking and the generation of masses for the fundamental particles in the standard model (SM), electroweak gauge bosons, leptons, and quarks, will have been taken. In the near future, the search for Higgs bosons will be carried out at hadron colliders, the proton-antiproton collider Tevatron [2] with a center-of-mass (c.m.) energy of 2 TeV, followed by the proton-proton Cern Large Hadron Collider (LHC) [3] with 14 TeV. Analyses of precision electroweak data [4] set the focus on $M_H \lesssim 200$ GeV as the preferential Higgs mass range in the SM, although a firm prediction without escape roads is not possible [5].

Various channels can be exploited at hadron colliders to search for a Higgs boson in the intermediate mass range. Among these channels Higgs radiation off top quarks [6] plays an important role:

$$p\bar{p}/pp \to t\bar{t}H + X \quad \text{via } q\bar{q}, gg \to t\bar{t}H\,. \qquad (1)$$

Although the expected rate is low at the Tevatron, samples of a few very clean events could be observed for Higgs masses below 140 GeV, while this channel becomes very demanding above [7]. At the LHC, associated production of the Higgs boson with top quarks is an important search channel for Higgs masses below ~125 GeV. Moreover, analyzing the $t\bar{t}H$ production rate at the LHC can provide information on the top-Higgs Yukawa coupling, assuming standard decay branching ratios [8], before model independent precision measurements of this coupling are performed at e^+e^- colliders [9].

Predictions for the cross sections (1), which are based on the leading order (LO), are plagued by considerable uncertainties due to the strong dependence on the renormalization and factorization scales, introduced by the QCD coupling and the parton densities (see the figures below). While estimates of radiative corrections were given earlier in the "effective Higgs approximation" (EHA) [10], in this Letter we present the first complete calculation of the QCD corrections at next-to-leading order (NLO), which reduces the spurious scale dependence significantly and leads to stable predictions for the cross sections.

The Born diagrams, generic examples of which are displayed in Fig. 1(a), are supplemented in NLO by virtual gluon-exchange diagrams [Fig. 1(b)], running in

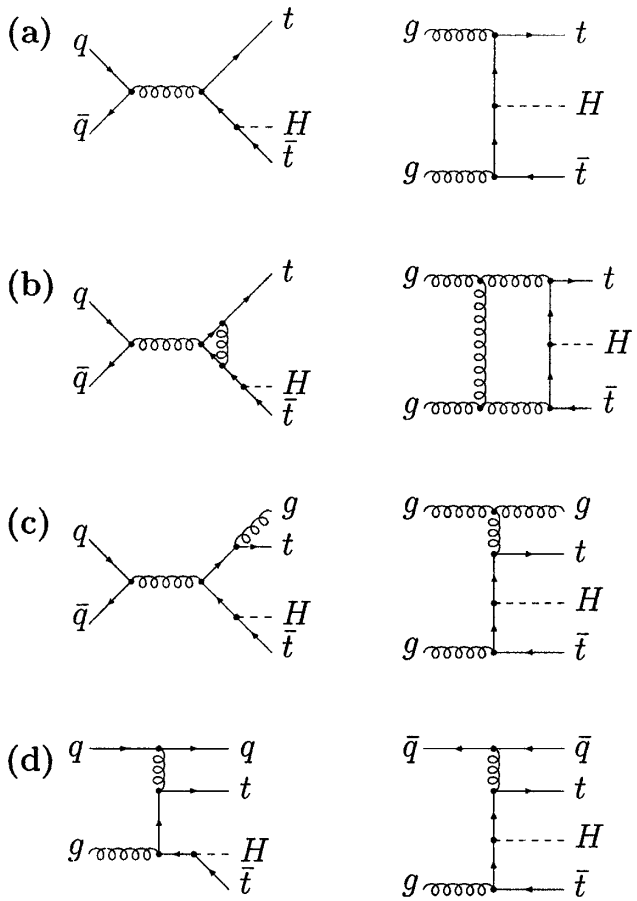

FIG. 1. A generic set of diagrams (a) for the Born level, (b) for virtual gluon exchange, (c) gluon radiation, and (d) parton splitting in the subprocesses $q\bar{q}$, $gg \to t\bar{t}H$, etc.

complexity up to pentagons, by gluon radiation [Fig. 1(c)], and by parton splitting [Fig. 1(d)]. The latter two add incoherently to the virtual corrections.

Dimensional regularization has been adopted for isolating the ultraviolet, infrared, and collinear singularities. Renormalization and factorization are performed in the $\overline{\rm MS}$ scheme with the top mass defined on shell. The top quark is decoupled from the running of the strong coupling $\alpha_s(\mu)$. For the evaluation of the $p\bar{p}/pp$ cross sections we have adopted the CTEQ4L and CTEQ4M [11] parton densities at LO and NLO, corresponding to the QCD parameters $\Lambda_5^{\rm LO} = 181$ MeV and $\Lambda_5^{\overline{\rm MS}} = 202$ MeV at the one- and two-loop levels of $\alpha_s(\mu)$, respectively. The strength of the SM Yukawa coupling is fixed by $g_{ttH} = m_t/v$, where $v = 246$ GeV is the vacuum-expectation value of the Higgs field, and the top-quark mass is set to $m_t = 174$ GeV.

The most complicated one-loop diagrams are the pentagons, both analytically and numerically. To calculate a five-point integral $E^{(D)}$ in D dimensions, the singularity structure $E_{\rm sing}^{(D)}$ in D dimensions is determined first. The singular part $E_{\rm sing}^{(D)}$ is given entirely by three-point subintegrals. The difference $E^{(D)} - E_{\rm sing}^{(D)}$ is finite and regularization-scheme independent. Therefore it can be calculated in the convenient mass regularization scheme in four dimensions. The original integral $E^{(D)}$ then reads

$$E^{(D)} = E_{\rm sing}^{(D)} + [E^{({\rm mass};D=4)} - E_{\rm sing}^{({\rm mass};D=4)}] \qquad (2)$$

in the limits $D \to 4$ and mass $\to 0$. Since $E^{({\rm mass};D=4)}$ can be expressed in terms of four-point functions [12], the D-dimensional five-point integral $E^{(D)}$ is finally reduced to three- and four-point functions. These integrals and their tensor structures can be treated according to standard methods [13]. Numerical instabilities, caused by vanishing Gram determinants near the phase-space boundary, can be controlled by careful extrapolation out of the safe inner phase-space domains. (Technical details will be presented in a subsequent publication.)

To extract the singularities of the real part of the NLO corrections $\sigma^{\rm real}$, a generalization of the dipole subtraction formalism [14] to massive quarks [15] has been adopted (see also Ref. [16]). The singularities of the cross section $\sigma^{\rm real}$ are mapped onto a suitably chosen auxiliary cross section $\sigma^{\rm sub}$ which is still simple enough so that the singular regions in phase space can be integrated out analytically, while the difference $\sigma^{\rm real} - \sigma^{\rm sub}$ can safely be integrated numerically in four dimensions. The auxiliary cross section $\sigma^{\rm sub}$ can be decomposed into a part $\sigma_1^{\rm sub}$ that, defined on configurations with LO kinematics, cancels the soft and collinear singularities of the virtual corrections $\sigma^{\rm virtual}$, and a second part $\sigma_2^{\rm sub}$ that includes the singularities from initial-state parton splitting, which are absorbed in the renormalization $\sigma^{\rm part}$ of the parton densities. Thus the total NLO correction $\Delta\sigma^{\rm NLO}$ can be written as the sum

$$\Delta\sigma^{\rm NLO} = [\sigma^{\rm real} - \sigma^{\rm sub}] + [\sigma^{\rm virtual} + \sigma_1^{\rm sub}] + [\sigma^{\rm part} + \sigma_2^{\rm sub}], \qquad (3)$$

in which each bracket is separately finite. (As an independent cross check the phase-space slicing method has been applied to the subchannel $q\bar{q} \to t\bar{t}H$, which dominates at the Tevatron. The results obtained by the slicing and the subtraction techniques are in mutual agreement.)

The results for the Tevatron are displayed in Figs. 2(a) and 2(b). For a Higgs mass between 100 and 150 GeV, the cross section varies between about 10 and 2 fb, the central value $\mu \to \mu_0 = (2m_t + M_H)/2$ chosen for the renormalization and factorization scales. In NLO the theoretical prediction is remarkably stable with very little variation for μ between $\sim\mu_0/3$ and $\sim 3\mu_0$, in contrast to the Born approximation for which the production cross section changes by more than a factor of 2 within the same

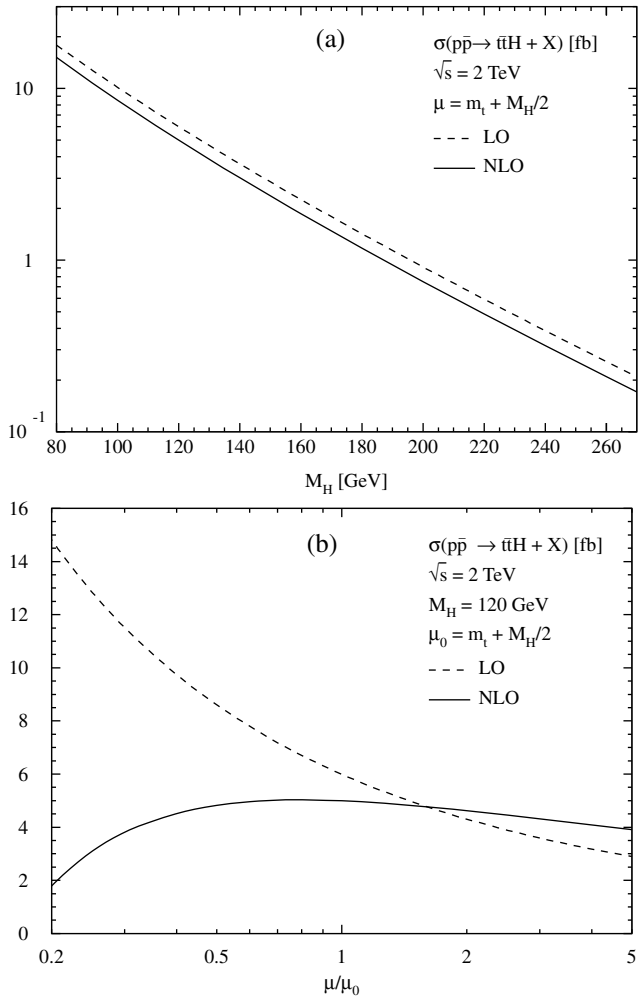

FIG. 2. (a) The cross section for $p\bar{p} \to t\bar{t}H + X$ at the Tevatron in LO and NLO approximation, with the renormalization and factorization scales set to $\mu = m_t + M_H/2$; (b) variation of the cross section with the renormalization and factorization scales for a fixed Higgs-boson mass $M_H = 120$ GeV.

interval. The cross section at the Tevatron is strongly dominated by the $q\bar{q}$ channel. Although a consistent study of the scale dependence requires the inclusion of the gq, $g\bar{q}$, and gg initial states, the effect of these channels is small. If μ is chosen too low, large logarithmic corrections spoil the convergence of perturbation theory, and the NLO cross section would even turn negative for $\mu \lesssim \mu_0/5$.

As is apparent from Fig. 2(b), the K factor, $K = \sigma_{\rm NLO}/\sigma_{\rm LO}$ with the cross sections $\sigma_{\rm LO}$ and $\sigma_{\rm NLO}$ calculated consistently in lowest and next-to-leading order, respectively, varies from $\sim$0.8 at the central scale $\mu = \mu_0$ to $\sim$1.0 at the threshold scale $\mu = 2\mu_0$. The small K factor can be understood intuitively in the fragmentation picture proposed in Ref. [10]. The average c.m. energy $\langle\sqrt{\hat{s}}\rangle$ for the subprocess $q\bar{q} \to t\bar{t}H$ at the Tevatron is about 650 GeV, i.e., sufficiently above the threshold region, so that the EHA of Ref. [10] can be used at least at a qualitative level, as confirmed earlier for $e^+e^- \to t\bar{t}H$ [9]. For $M_H^2 \ll m_t^2 \ll \langle\sqrt{\hat{s}}\rangle^2$, the probability for the hadronic process is decomposed into the product of probabilities for $t\bar{t}$ production and subsequent fragmentation $t \to t + H$. As a result, the relative QCD corrections take the form $\delta = \delta[p\bar{p} \to t\bar{t}] + \delta[t \to t + H]$. With $\delta[p\bar{p} \to q\bar{q} \to t\bar{t}] \sim -\alpha_s/2\pi$ [17] and $\delta[t \to t + H] \sim -4\alpha_s/\pi$ for small energies of the Higgs boson, the sum of the terms $\delta \sim -9\alpha_s/2\pi$ is negative and the K factor is predicted below unity in this limit. Integrating over the entire Higgs spectrum, the numerical evaluation yields $K_{\rm EHA} \sim 0.7$, which is nicely compatible with the result $K \sim 0.8$ of the full $\mathcal{O}(\alpha_s)$ calculation.

Near threshold, $\sqrt{\hat{s}} \gtrsim 2m_t + M_H$, the QCD corrections are enhanced by Coulombic gluon exchange between the top and antitop quark in the final state. This Sommerfeld rescattering correction [18] increases inversely proportional to the maximum $t/\bar{t}$ velocity $\hat{\beta}_t^{\rm max} \sim \sqrt{(\sqrt{\hat{s}} - M_H)^2 - 4m_t^2}/2m_t$ in the $t\bar{t}$ c.m. frame: $\delta_{\rm Coul}(\hat{s}) = C \times (\pi\alpha_s/2)\langle 1/\hat{\beta}_t\rangle = C \times 8\alpha_s/3\hat{\beta}_t^{\rm max}$. If the $t\bar{t}$ pair is generated in a color-singlet state, the quark and antiquark attract each other, and with $C_1 = +4/3$ the correction is positive. This leads to a strong enhancement of the $e^+e^- \to t\bar{t}H$ annihilation cross section near threshold [9]. By contrast, if the $t\bar{t}$ pair is generated in a color-octet state, the force is repulsive, and with $C_8 = -1/6$ the correction is negative and relatively small. This applies to the dominant channel at the Tevatron, $q\bar{q} \to t\bar{t}H$, which is mediated by s-channel color-octet gluon exchange. As a consequence, the destructive Coulomb interference term amplifies the reduction of the cross section.

The improvement of the prediction for the cross section at the LHC [Figs. 3(a) and 3(b)] is similarly striking. However, the gluon initial states give rise to increased gluon radiative corrections (which will be improved by resummation techniques in the future). For the central renormalization/factorization scale μ_0 we obtain $K \sim 1.2$,

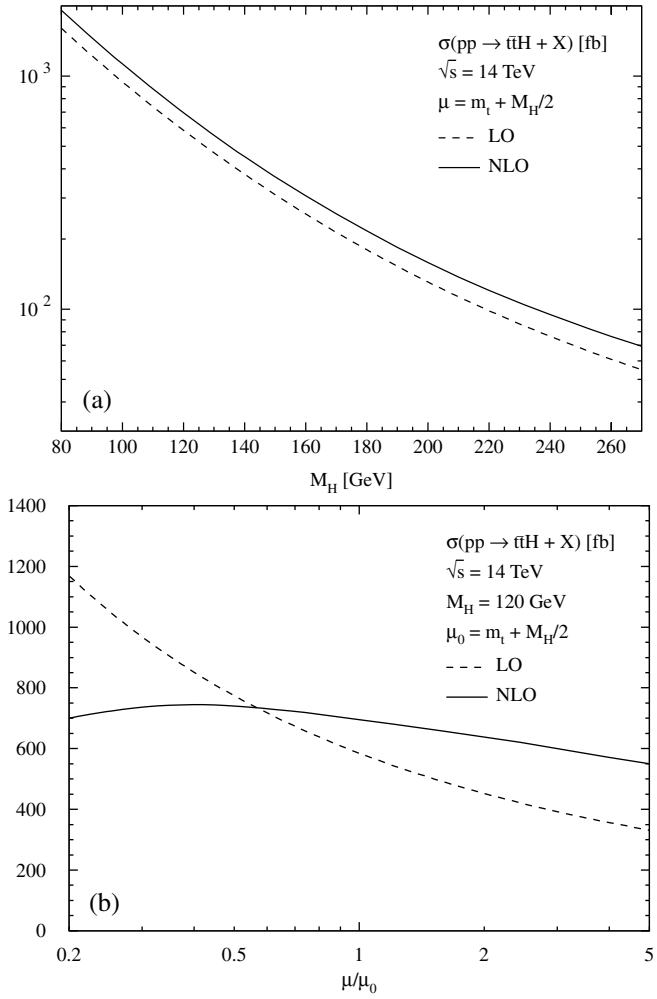

FIG. 3. Analysis of $pp \to t\bar{t}H + X$ at the LHC; (a) production cross section and (b) renormalization/factorization-scale dependence (parameters as specified in Fig. 2).

increasing to $\sim$1.4 at the threshold value $\mu = 2\mu_0$. These values are nearly independent of M_H in the relevant Higgs mass range.

The K factor at the LHC can be estimated in the fragmentation picture [10], since the average subenergy $\langle\sqrt{\hat{s}}\rangle \sim 830$ GeV is relatively high at the LHC. With the dominant gg production channel, the sum of $\delta[pp \to gg \to t\bar{t}] \sim +11\alpha_s/\pi$ and $\delta[t \to t + H] \sim -4\alpha_s/\pi$ for the QCD corrections comes now with opposite signs, but the positive correction to the $t\bar{t}$ production in the gg channel more than compensates the negative correction to the fragmentation, leading finally to $\delta \sim +7\alpha_s/\pi$. Taking into account the different renormalization and factorization scales, the estimate for the K factor in Ref. [10] is recognized compatible at the qualitative level with the full NLO result.

In summary, the strong scale dependence of the Born cross sections in the reactions $pp/p\bar{p} \to t\bar{t}H$, which provide important search channels for the SM Higgs boson, requires the improvement by NLO QCD corrections. In

agreement with a qualitative fragmentation picture, the K factor at the Tevatron is slightly below unity, i.e., varying between ~ 0.8 and ~ 1.0 for renormalization and factorization scales $\mu = \mu_0$ and $2\mu_0$, with $2\mu_0$ denoting the threshold c.m. energy of the parton subprocesses. Similarly, the K factor varies between ~ 1.2 and ~ 1.4 for the same scale at the LHC. Most important, in contrast to the Born approximation, the predictions for the cross sections including NLO QCD corrections are stable when the renormalization and factorization scales are varied so that the improved cross sections can serve as a solid base for experimental analyses at the Tevatron and the LHC.

The analysis of the subprocess $q\bar{q} \to t\bar{t}H$ at the Tevatron has been compared with the parallel calculation of Ref. [19]; the results are in agreement.

We thank Sally Dawson and Laura Reina for their cooperation. M. K. thanks Keith Ellis for discussions and the DESY Theory Group for its hospitality. This work was supported by the European Union under Contract No. HPRN-CT-2000-00149.

[1] P. W. Higgs, Phys. Lett. **12**, 132 (1964); Phys. Rev. Lett. **13**, 508 (1964); Phys. Rev. **145**, 1156 (1966); F. Englert and R. Brout, Phys. Rev. Lett. **13**, 321 (1964); G. S. Guralnik, C. R. Hagen, and T. W. Kibble, Phys. Rev. Lett. **13**, 585 (1964).

[2] M. Carena *et al.,* hep-ph/0010338.

[3] ATLAS Collaboration, Technical Design Report No. CERN-LHCC 99-14, 1999; CMS Collaboration, Technical Report No. CERN-LHCC 94-38, 1994.

[4] LEP Collaboration, LEP Electroweak Working Group, and SLD Heavy Flavor and Electroweak Group, hep-ex/0103048; T. Kawamoto, hep-ex/0105032; E. Tournefier, hep-ex/0105091; J. Erler, hep-ph/0102143.

[5] M. S. Chanowitz, hep-ph/0104024; J. A. Bagger, A. F. Falk, and M. Swartz, Phys. Rev. Lett. **84**, 1385 (2000); M. E. Peskin and J. D. Wells, hep-ph/0101342.

[6] Z. Kunszt, Nucl. Phys. **B247**, 339 (1984); W. J. Marciano and F. E. Paige, Phys. Rev. Lett. **66**, 2433 (1991); J. F. Gunion, Phys. Lett. B **261**, 510 (1991).

[7] J. Goldstein, C. S. Hill, J. Incandela, S. Parke, D. Rainwater, and D. Stuart, Phys. Rev. Lett. **86**, 1694 (2001).

[8] M. Beneke *et al.,* Report No. CERN 2000-04, hep-ph/0003033; V. Drollinger, hep-ex/0105017.

[9] A. Djouadi, J. Kalinowski, and P. M. Zerwas, Z. Phys. C **54**, 255 (1992); S. Dittmaier, M. Krämer, Y. Liao, M. Spira, and P. M. Zerwas, Phys. Lett. B **441**, 383 (1998); S. Dawson and L. Reina, Phys. Rev. D **59**, 054012 (1999).

[10] S. Dawson and L. Reina, Phys. Rev. D **57**, 5851 (1998).

[11] CTEQ Collaboration, H. L. Lai *et al.,* Phys. Rev. D **55**, 1280 (1997).

[12] D. B. Melrose, Muovo Cimento **40**, 181 (1965).

[13] G. 't Hooft and M. Veltman, Nucl. Phys. **B153**, 365 (1979); G. Passarino and M. Veltman, Nucl. Phys. **B160**, 151 (1979); W. Beenakker and A. Denner, Nucl. Phys. **B338**, 349 (1990); A. Denner, U. Nierste, and R. Scharf, Nucl. Phys. **B367**, 637 (1991).

[14] S. Catani and M. H. Seymour, Phys. Lett. B **378**, 287 (1996); Nucl. Phys. **B485**, 291 (1997); *ibid.* **B510**, 291E (1997).

[15] S. Catani, S. Dittmaier, M. H. Seymour, and Z. Trócsányi (to be published).

[16] S. Dittmaier, Nucl. Phys. **B565**, 69 (2000); S. Catani, S. Dittmaier, and Z. Trócsányi, Phys. Lett. B **500**, 149 (2001); L. Phaf and S. Weinzierl, J. High Energy Phys. **04**, 006 (2001).

[17] P. Nason, S. Dawson, and R. K. Ellis, Nucl. Phys. **B303**, 607 (1988); Nucl. Phys. **B327**, 49 (1989); W. Beenakker, H. Kuijf, W. L. van Neerven, and J. Smith, Phys. Rev. D **40**, 54 (1989); W. Beenakker, W. L. van Neerven, R. Meng, G. A. Schuler, and J. Smith, Nucl. Phys. **B351**, 507 (1991).

[18] A. Sommerfeld, *Atombau und Spektrallinien* (F. Vieweg und Sohn, Braunschweig, 1939), Vol. II, p. 457.

[19] L. Reina and S. Dawson, preceding Letter, Phys. Rev. Lett. **87**, 201804 (2001); L. Reina, S. Dawson, and D. Wackeroth, Report No. FSU-HEP-2001-0602, hep-ph/0109066.